Received: 18 December 2018 | Revised: 22 April 2019 | Accepted: 24 April 2019

DOI: 10.1111/cas.14031

ORIGINAL ARTICLE

WILEY Cancer Science

Loss of PTPN4 activates STAT3 to promote the tumor growth in rectal cancer

Bing-Dong Zhang[1] | Yue-Rui Li[1] | Li-Dan Ding[2] | Yin-Yin Wang[2] | Hong-Yi Liu[1] | Bao-Qing Jia[1]

[1]Chinese PLA General Hospital, Beijing, China

[2]State Key Laboratory of Membrane Biology, Department of Basic Medical Sciences, School of Medicine, Tsinghua University, Beijing, China

Correspondence
Bao-Qing Jia, General Surgery II Department, Chinese PLA General Hospital, 28th Haidian District, Beijing 100853, China.
Email: jiabaoqing@301hospital.com.cn

Funding information
National Natural Science Foundation of China, Grant/Award Number: 81772929

Abstract

Colorectal cancer (CRC) is one of the most common types of malignant tumor. Many genetic factors have been proved to show high association with the occurrence and development of CRC and many mutations are detected in CRC. PTPN4/PTP-MEG1 is a widely expressed non–receptor protein tyrosine phosphatase. Over the past three decades, PTPN4 has been demonstrated in the literature to participate in many biological processes. In this study, we identified a nonsense mutation of PTPN4 with a mutation ratio of 90.90% from 1 case of rectal cancer, leading to loss of function in PTPN4 gene. Several somatic mutations occurred in 5/137 rectal cancer samples from The Cancer Genome Atlas Rectum Adenocarcinoma (TCGA READ) database. Interestingly, we found that PTPN4 negative cytoplasm staining was more prone to lymphatic metastasis (N = 50, P = 0.0153) and low expression of PTPN4 in rectal cancer was highly associated with poor prognosis. Overexpression of PTPN4 suppressed the cell growth, and moreover, the loss of PTPN4 accelerated cell growth and boosted clonogenicity of CRC cells. Furthermore, we revealed that the deletion of PTPN4 promoted the tumor formation of NCM460 cells in vivo. In terms of the molecular mechanism, we demonstrated that PTPN4 dephosphorylates pSTAT3 at the Tyr705 residue with a direct interaction and suppresses the transcriptional activity of STAT3. In summary, our study revealed a novel mechanism that the tumorigenesis of colorectal cancer might be caused by the loss of PTPN4 through activating STAT3, which will broaden the therapy strategy for anti–rectal cancer in the future.

KEYWORDS
nonsense mutation, phosphatase, PTPN4/PTP-MEG1, rectal cancer, STAT3

1 | INTRODUCTION

Colorectal cancer (CRC), accounting for approximately 10% of all cancer cases, is one of the most common types of malignant tumor, leading to more than one-third of rectal-related incidences. Although several studies have revealed that environmental and genetic factors contribute to the occurrence and development of CRC, many mutations are detected in CRC, which play important roles in tumorigenesis and progression of the tumor. Studies have revealed that many genes were frequently mutated in CRC, including TP53, APC, KRAS, PIK3CA, NRAS, FBXW7, SMAD4 and TCF7L2.[1] These genetic mutations alter signaling pathways such as Ras/Erk1/2, Src, JAK/STAT,

JNK, NF-κB, Wnt and PTEN/PI3K/AKT, controlled by protein tyrosine kinases and protein tyrosine phosphatases (PTP).[2]

In human beings, there are more than 100 phosphatases genes,[3] which can be divided into 4 distinct classes according to amino acid sequence in the phosphatase catalytic domains. Among these phosphatases, the largest class, Class I, can be divided into receptor and non–receptor PTP.[3] PTPN4/PTP-MEG1, a widely expressed non–receptor PTP, contains FERM, PDZ and C-terminal catalytic domains. In 1991, PTPN4 gene was first cloned with a human megakaryoblastic cell line (MEG-01) and umbilical vein endothelial cell cDNA libraries, which is the reason that PTPN4 was also referenced as MEG: PTPMEG or PTPMEG1.[4] PTPN4 localizes in the cytoplasm and the plasma membrane. The active form of PTPN4 consists of the PDZ and PTP domains.[5]

Emerging studies have shown that PTPN4 participates in many biological processes. The overexpression of PTPN4 affects cell growth and colony formation in soft agar of COS-7 cells and suppresses CrkI-mediated cell growth and mobility in HEK293T cells.[6,7] However, other studies have addressed that PTPN4 suppresses the cell apoptosis of neuroblastoma and glioblastoma cell lines in a PDZ-PDZ binding motifs-dependent manner. Besides the regulation of cell proliferation and apoptosis, PTPN4 also plays an important part in innate immune responses by suppressing tyrosine phosphorylation of TRAM and the TCR ITAM. Moreover, other studies have suggested that PTPN4 was highly associated with learning, spatial memory and cerebellar synaptic plasticity.[8,9] In these studies, 5 endogenous partners of PTPN4 have been reported: (i) mitogen-activated protein kinase (MAPK) p38γ; (ii) glutamate receptor δ2 and ε subunits; (iii) TRIF-related adaptor molecule TRAM; (iv) T-cell receptor ξ subunit; and (v) oncoprotein CrkI. However, it remains unclear whether PTPN4 participates in the CRC tumorigenesis and the detailed mechanism of PTPN4 regulation in CRC still needs to be elucidated.

In this study, we identified a nonsense mutation of PTPN4 from 1 case of rectal cancer by exome capture DNA sequencing, leading to loss of function in PTPN4 gene. Low expression of PTPN4 in rectal cancer is associated with poor prognosis, and overexpression of PTPN4 suppresses the cell growth of colorectal cancer cells. Moreover, the deletion of PTPN4 promotes the cell proliferation ability and tumor formation of colorectal cancer cells. In terms of molecular mechanisms, we revealed that PTPN4 dephosphorylates pSTAT3 at the Tyr705 residue with a direct interaction, which might provide novel targets for the therapy of CRC.

2 | MATERIALS AND METHODS

2.1 | Cell culture, antibodies and plasmid construction

DLD-1, NCM460 (one immortalized colorectal epithelial cell line) and HEK293T cells were obtained from ATCC and maintained in our laboratory according to the recommendation of ATCC. Stable cell lines for the knockdown of PTPN4 by shRNA were generated based on DLD-1, which were infected with lentivirus and selected by puromycin at 2 μg/mL. Stable cell line for knockout of PTPN4 by CRISPR Case9 was generated based on NCM460 and screened using FACS. The guide RNA used for knocking out of PTPN4 were 5′-TCTAGACAAATCAGCTTGAA-3′ and 5′-GGTTACGACCATCTTCAGTT-3′, which were selected from http://crispr.mit.edu/ and subcloned into the PX458M plasmid.

Anti–PTPN4 antibody was purchased from Sigma-Aldrich (St. Louis, MO, USA) (HPA019351) and Abcam (Cambridge, MA, USA) (ab200363). Anti–phosphotyrosine antibody (4G10) was purchased from Millipore (Hong Kong, China). Anti–HA, anti–Erk1/2, anti–pErk1/2 and protein G/A plus agarose beads were purchased from Santa Cruz Biotechnology (Santa Cruz, CA, USA). Anti–pSTAT3 (Tyr705), anti–pSTAT3 (Ser727), anti–STAT3, anti–Ki-67, anti–β-Actin antibodies and anti–rabbit IgG (H+L), F(ab′)2 Fragment was purchased from Cell Signaling Technology (Shanghai, China). Goat anti–Mouse IgG (H+L) Highly Cross-Adsorbed Secondary Antibody, Alexa Fluor 546 was purchased from Thermo Fisher Scientific (Shanghai, China). Plasmids including 3Flag-PTPN4 and 3HA-PTPN4-IRES-EGFP were expression vectors constructed based on pcDNA3.0-3Flag and pCDH-CAG-3HA-IRES-EGFP, respectively, for human PTPN4 and PTPN4 c.549dupT.

2.2 | Clinical samples

Eleven primary paired rectal cancer samples including tumor and adjacent non–tumorous samples were randomly selected from the Chinese PLA General Hospital (Beijing) and used for the western blot. The pathological type was confirmed by the pathologists. Twenty-five TNM stage II and 25 TNM stage III rectal cancer patients who underwent surgical treatment were selected for immunohistochemical analysis. The Ethics Committee of the Chinese PLA General Hospital (Beijing) approved the tissue collection with informed consent.

2.3 | Exome capture, library construction, sequencing and somatic mutation identification

Whole-exome capture DNA sequencing service was provided by GenomiCare Biotechnology (Shanghai). Genomic DNA was fragmented and hybridized to Agilent SureSelect Human All Exome kit V5. Exome-enriched shotgun libraries were sequenced on the Illumina X platform, and pair-end reads with size of 150 *2 bp were generated. Image analysis and base calling were performed with Illumina CAVSAVR version 1.8, using default parameters. After removing reads with sequence matching, the sequencing adaptors and low-quality reads with exact match, high-quality reads were aligned to the NCBI human reference genome hg19 using Burrows-Wheeler Aligner tools. Reads in fastq format were initially processed with Genome Analysis Toolkit (GATK) version 3.5. Localized insertion deletion (InDel) realignments were performed using GATK. Regions that needed to be realigned were identified using the GATK Realigner Target Creator (https://software.broadinstitute.org/gatk/). For single nucleotide variants (SNV) detection, the MuTect algorithm was used to identify

candidate SNV in xenografts that exhibited drug resistance based on comparison to control xenografts from the same patient. The ANNOVAR software (http://annovar.openbioinformatics.org/en/latest/) was used for SNV annotation. The possible effects of non-synonymous mutations on the encoded proteins were predicted using the dbNSFP database, version 3.1 (http://varianttools.sourceforge.net/Annotation/DbNSFP), by collating outputs from the SIFT32 and Polyphen2 prediction programs. Candidate somatic resistance InDels were identified using InDelocator (http://www.broadinstitute.org/cancer/cga/indelocator) based on comparisons to control xenografts from the same patient. Candidate InDels were only considered when they were supported by ≥5 reads and when the ratio of the number of supporting reads to the maximum breakpoint read depth was >.05. All InDel calls were manually reviewed using the Integrative Genomics Viewer (http://software.broadinstitute.org/software/igv/) before being annotated with ANNOVAR.

2.4 | Immunohistochemical staining

Formalin-fixed, paraffin-embedded tissue blocks were cut into 4-μm paraffin sections, followed by immunohistochemical analysis. The slides were heated in a tissue-drying oven for 40 minutes at 65°C, followed by deparaffinization in xylene and rehydration in a graded alcohol series. The slides were incubated in sodium citrate solution (pH 6.0) and heated in a boiling water bath for 20 minutes for antigen retrieval. After endogenous peroxidases were blocked by soaking the slides in 3% H_2O_2, the slides were incubated with anti–PTPN4 antibody (Abcam, Cambridge, MA, USA, ab200363, 1:50) in a humidity chamber at 4°C overnight. We washed the slides with PBS 3 times, and applied the EnVision Kit (Dako, Glostrup, Denmark) to the sections on the slides and incubated in a humidified chamber at room temperature for 30 minutes. Signal detection was performed using diaminobenzidine in the EnVision Kit (Dako). All the slides were examined under a microscope by 2 blinded pathologists. According to the degree of positive staining, positive intensity can be divided into negative (–), weak positive (+), medium positive (++) and strong positive (+++). All patients gave informed consent for participation in the study.

2.5 | Western blotting

Cells were harvested and homogenized in RIPA buffer (Cell Signaling Technology, Shanghai, China), followed by determination of protein concentration using the BCA Kit (Life Technologies, Shanghai, China). Proteins were resolved by 10% SDSPAGE, and then transferred to .45-mm polyvinylidene difluoride (PVDF) membranes. The membranes were blocked in 5% skimmed milk in TBS with Tween 20 (TBST) at 37°C for 1 hour and incubated with primary antibody at 4°C overnight. The PVDF membranes were rigorously washed with TBST and subjected to secondary antibody hybridization. The protein bands were visualized using enhanced chemiluminescence (Millipore, Hong Kong, China).

2.6 | RT-PCR

The primers used for PTPN4 amplification were 5′-ATCTCCACC GGGAACTCCTA-3′ and 5′-CGCTTGGGGAAGTATGAACCA-3′. The primers for GAPDH amplification were 5′-AACGTGTCAGTGGTGGA CCTG-3′ and 5′-AGTGGGTGTCGCTGTTGAAGT-3′. The RT-PCR for the detection of mRNA levels of PTPN4 and GAPDH included 28 cycles of PCR amplification with 94°C for 30 seconds, 55°C for 30 seconds and 72°C for 40 seconds. The RT-PCR products were analyzed with 1% agarose gels and observed under ultraviolet light (Bio-Rad).

2.7 | CCK proliferation assay

Cells were counted by FACS and then seeded into 96-well plates at 2×10^3/well. CCK-8 (Dojindo, Shanghai, China) reagent was diluted and added to the wells according to the protocol. Absorbance at 450 nm was documented with a reference filter of 570 nm using a microplate reader (Molecular Devices, San Jose, CA, USA). Data were collected for 7 days.

2.8 | Immunofluorescence staining

HEK293T cells were seeded on coverslips. After transfection with 3Flag-PTPN4 for 24 hours, the cells were fixed with 4% paraformaldehyde for 20 minutes and perforated with .3% Triton X-100 for 10 minutes. After blocking with 10% FBS for 50 minutes, cells were incubated with anti–Flag and anti–STAT3 antibodies overnight at 4°C, followed with incubation with the secondary antibodies for 1 hour. Stained cells were visualized using a confocal laser scanning microscope with co–localization of the 2 proteins indicated by a merged image.

Wild-type and $PTPN4^{KO}$ NCM460 cells were seeded on coverslips. After 24 hours of serum-free starvation, cells were stimulated with epidermal growth factor (EGF) (25 ng/mL) for 5 minutes and cultured in serum-free medium for 0, 10, 20 and 30 minutes. After treatment, cells were fixed with 4% paraformaldehyde for 20 minutes and perforated with .3% Triton X-100 for 10 minutes. After blocking with 10% FBS for 50 minutes, cells were incubated with anti–STAT3 antibody overnight at 4°C, followed with incubation with the secondary antibodies for 1 hour. Stained cells were visualized using a confocal laser scanning microscope.

2.9 | Flow cytometric analyses

HEK293T, DLD-1 and NCM460 cells were seeded in 6-well plates. After digestion and suspension, cells were fixed with 70% ethanol overnight at 4°C. Then cells were re-suspended in 1-mL DAPI solution (.1% [v/v] Triton X-100, 1 μg/mL DAPI) and incubated at room temperature for 30 minutes. Each sample was tested for 30 000 cells by flow cytometry.

2.10 | Luciferase assay

HEK293T cells were plated in 24-well plates the day before transfection. A total of .05 μg pAPRE-luc or .1 μg pFA-luc plus .1 μg pFR-ELK1

reporter plasmid together with 5 ng of pRL-TK was transfected. The constructed plasmid overexpressing PTPN4 was co–transfected at an amount of .4 μg/well. Four hours after transfection, HEK293T cells were treated with EGF (25 ng/mL) for 6 hours after starvation for 24 hours, and luciferase assays were conducted with a dual-luciferase reporter assay system (Vigofect, Beijing, China).

2.11 | Colony formation assay

Cells were plated in 6-well plates at a density of 500 or 1000 cells/well. After culturing for 10 days, cells were fixed with methanol for 10 minutes and incubated with .1% crystal violet (Sigma) for 10 minutes at room temperature. The number of colonies was counted by Image J.

2.12 | Tumorigenesis assay

NCM460 cells (1×10^7 cells/mouse) were injected subcutaneously into the right or left dorsal flank of 6-week-old BALB/c nude mice with control cells and experimental cells. When tumors were approximately 1.0 cm in diameter, mice were killed and tumor tissues were collected. This protocol followed the guidelines and regulations on animal health and ethics and was approved by the animal health and ethics committee in the Chinese PLA Medical School.

2.13 | Immunoprecipitation assay

Lysates were subjected directly to immunoblot analysis and immunoprecipitated overnight with the indicated antibodies. Immune complexes were incubated with Protein G/A PLUS-Agrose (sc-2002, Santa Cruz Biotechnology) and washed in cell lysis buffer, followed by immunoblotting.

2.14 | The construction of lentivirus plasmids

Short hairpin RNA (shRNA) was designed to downregulate PTPN4. The sequences were: 5′-GCTCCGAACAAATAGTAAATA-3′ (PTPN4-shRNA5), 5′-CCTTCTAATACTGCTGCCCTT-3′ (PTPN4-shRNA6), 5′-GCTGTATATGATGTAGTGGAA-3′ (PTPN4-shRNA7), 5′-CGTCATCAACACAAGCTAATA-3′ (PTPN4-shRNA8). Then, the sequences were inserted into pCDH-GLI-1-shRNA plasmids.

2.15 | Statistical analysis

Data were represented as mean ± SD. Significant differences between proportions were assessed using Fisher's exact test. Significant differences between 2 groups were determined using Student's *t* test. Significant differences between 3 groups were determined using one-way ANOVA. Survival analysis was performed using Kaplan-Meier method. All the analyses were conducted using SPSS 17.0 software. Statistical significance was defined as $P < 0.05$.

3 | RESULTS

3.1 | A nonsense mutation of PTPN4 is detected in 1 case of rectal cancer

A 47-year-old Chinese man, who was categorized as T4bN2aM1 stage IV in the NCCN guideline and diagnosed as having moderately-poorly differentiated adenosquamous carcinoma pathologically, underwent palliative resection for rectal cancer (Figure 1A). Whole-exome capture DNA sequencing was performed on the patient's tumor and leukocyte before PD-1 inhibitor treatment. After 3 months of treatment, the patient died of tumor progression. Surprisingly, a total of 98 somatic mutated genes were identified in the tumor tissue from the patient. Among these genes, a c.549dupT mutation of PTPN4 was identified with the highest mutation ratio of 90.90% (Figure 1B, Table S1). The mutation ratio exceeded 50%, so PTPN4 c.549dupT was a biallelic mutation. In consideration of the mutation ratio of 90.90%, the mutation of PTPN4 might occur in the early stage of tumorigenesis. A further sequence analysis demonstrated that this mutation enabled PTPN4 to obtain a premature stop codon, which was a kind of nonsense mutation. As a consequence of this mutation, the PTPN4 gene lost the C-terminal region containing the central PDZ, the C-terminal catalytic and part of the FERM domains (Figure 1C). To test this hypothesis, the plasmids of the wild-type PTPN4 and the truncated PTPN4 (PTPN4 c.549dupT), referred to as PTPN4 $^{c.549dupT}$, with a tag of 3Flag were constructed, and transfected into HEK293T cells. The results showed that the molecular weight of wild PTPN4 encoded by 3Flag-PTPN4 was >100 kDa, while protein encoded by 3Flag-PTPN4 $^{c.549dupT}$ was <30 kDa (Figure 1D). To examine the expression level of PTPN4 in this tumor tissue, a immunohistochemistry experiment was performed. The data demonstrated that the expression of PTPN4 was negative in the tumor tissue in comparison with the normal counterpart in the same slide (Figure 1E). Then we employed mutagenesis analyses for cancer genomics based on the TCGA READ database and found that several somatic mutations occurred in 5/137 rectal cancer samples, including 1 In_Frame_Del mutation, 5 missense mutation and 1 nonsense mutation (Figure 1F-1). Similar to BRAF, these PTPN4 somatic mutations occur mainly in patients with heavy tumor burden (Figure 1F-2). Taken together, all these data

FIGURE 1 A nonsense mutation of PTPN4 is identified in 1 case of rectal cancer. A, Computer tomography image of abdomen and pelvic cavity. Tumor (red triangle) thickened rectal wall (right side) and dilated the abdominal intestines (left side). B, PTPN4 had a mutation with the highest mutation ratio. A total of 98 somatic mutated genes were identified in 1 case of rectal cancer by exome capture DNA sequencing. C, A c.549dupT mutation enabled PTPN4 to obtain a premature stop codon. D, The molecular weight of wild PTPN4 encoded by 3Flag-PTPN4 is >100 kDa, while protein encoded by 3Flag-PTPN4 c.549dupT is <30 kDa. E, The expression of PTPN4 was negative in the rectal tumor tissue, whereas the positive PTPN4 was observed in the paired adjacent normal tissue. F, Several somatic mutations of PTPN4 were found in rectal cancer samples from the TCGA READ database. Somatic mutations in PTPN4 occur mainly in patients with heavy tumor burden

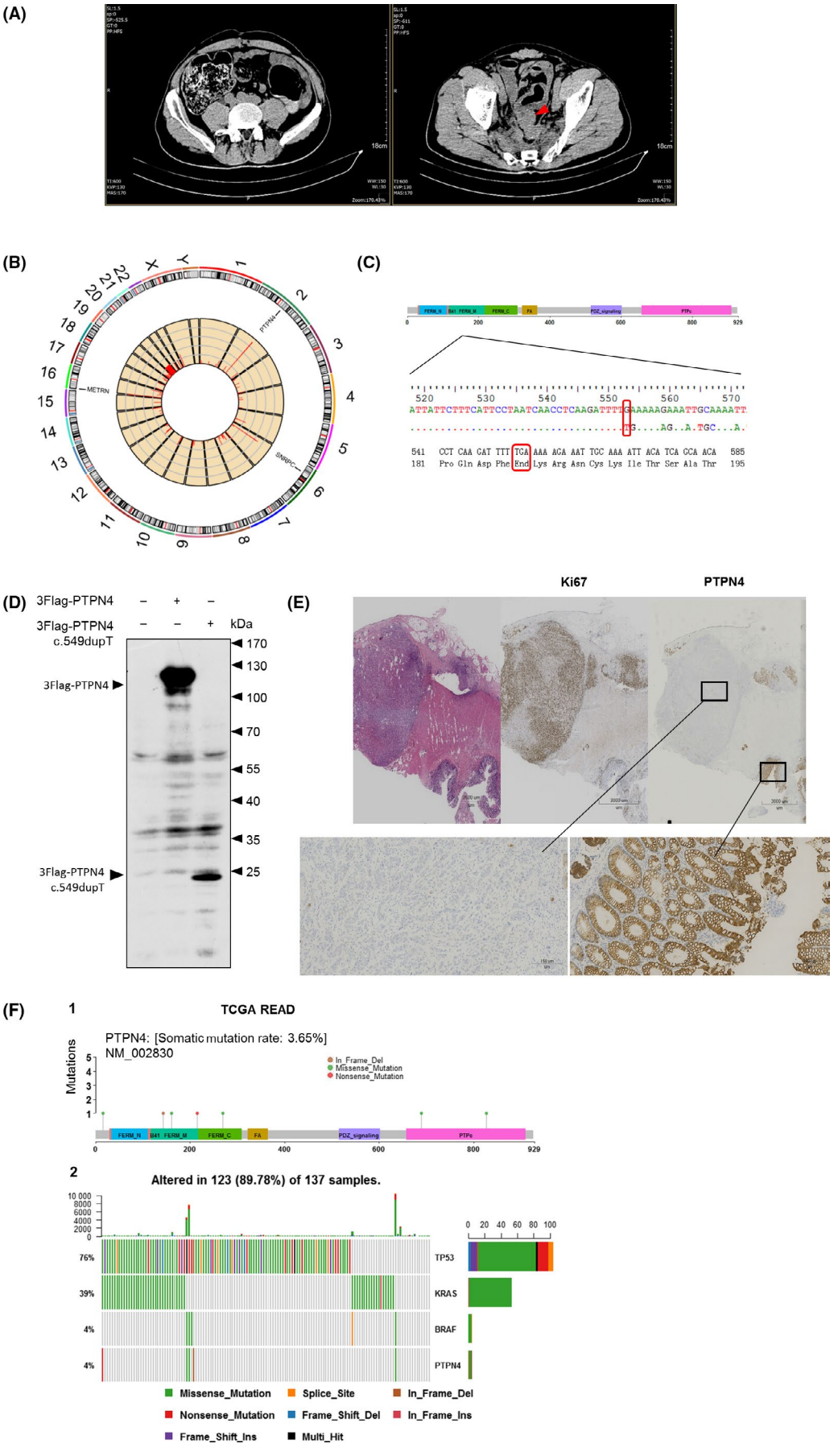
(A)
(B)
(C)
(D)
3Flag-PTPN4 – + –
3Flag-PTPN4 – – + kDa
3Flag-PTPN4 c.549dupT
3Flag-PTPN4
3Flag-PTPN4 c.549dupT
170
130
100
70
55
40
35
25
(E)
Ki67
PTPN4
(F)
1
TCGA READ
PTPN4: [Somatic mutation rate: 3.65%]
NM_002830
Mutations
In_Frame_Del
Missense_Mutation
Nonsense_Mutation
FERM_N
B41
FERM_M
FERM_C
FA
PDZ_signaling
PTPc
2
Altered in 123 (89.78%) of 137 samples.
76%
TP53
39%
KRAS
4%
BRAF
4%
PTPN4
Missense_Mutation
Splice_Site
In_Frame_Del
Nonsense_Mutation
Frame_Shift_Del
In_Frame_Ins
Frame_Shift_Ins
Multi_Hit

suggested that c.549dupT in PTPN4, a nonsense mutation with a mutation ratio of 90.90%, occurring in colorectal cancer, may play an essential role in the early stage of CRC tumorigenesis.

3.2 | Low expression of PTPN4 is associated with poor prognosis in rectal cancer

To explore the role of PTPN4 in the tumorigenesis and development of colorectal cancer, we evaluated the expression of PTPN4 in 11 primary rectal cancer tissues compared with their adjacent normal tissues by western blot. None of the patients received neoadjuvant therapy. Approximately 27% (3 in 11 samples) of primary rectal cancer tissues showed a significant downregulation of PTPN4, while around 36% (4 in 11 samples) of the primary rectal cancer tissues exhibited high expression of PTPN4 compared with their adjacent normal tissues (Figure 2A). It has been reported that lymph node metastasis is associated with poor prognosis.[10] In our study, although there is no significant difference in statistics between primary rectal cancer tissues and their adjacent normal tissues, patients with downregulated expression of PTPN4 (blue color) had more metastatic nodes (Figure 2B). To evaluate the association of PTPN4 with the clinicopathological features of patients with READ, we evaluated the PTPN4 protein expression in 50 READ tissue slides. We found that 68% (34/50) of READ tumors showed negative cytoplasm staining of PTPN4 and 32% (16/50) had moderate and weak staining (Figure 2C). More abundant expression of PTPN4 was observed in well-differentiated tumor tissue compared to poorly differentiated tumor tissue in several slides (Figure 2C-4). We also found that patients with PTPN4 negative cytoplasm staining were more prone to lymphatic metastasis (P = 0.0153, Figure 2D). To further confirm our findings, the mRNA expression of PTPN4 in rectal cancer samples from the TCGA database (https://genome-cancer.ucsc.edu) was analyzed. Curiously, PTPN4 was significantly increased in 9 rectal cancer samples compared with the paired adjacent normal samples (P = 0.0277) (Figure 2E). The upregulation of PTPN4 mRNA level was also observed in unpaired rectal cancer samples (n = 94) compared with normal samples (n = 10) from the TCGA READ cohort (P = 0.0015) (Figure 2F). We further analyzed the association of PTPN4 with pathological features and clinical outcomes of patients with rectal cancer. Ranking rectal cancer patients according to PTPN4 mRNA level and keeping the top 25% (High) and bottom 25% (Low) patients, no significant correlation was observed between PTPN4 expression and gender, age, and the TNM stage of rectal cancer patients (Table S2). However, the Kaplan-Meier analysis showed that a low level of PTPN4 mRNA was associated with a poor overall survival rate (Figure 2G). All these results indicated that PTPN4 may not be a driver gene in most rectal cancers. However, low expression of PTPN4 in rectal cancer is associated with poor prognosis.

3.3 | PTPN4 suppresses the proliferation ability of colorectal cancer cells

To explore the function of PTPN4 in CRC, we examined the effects of PTPN4 on growth characteristics of colorectal cancer cell line DLD-1 and NCM460 (an immortalized colorectal epithelial cell line) by colony formation assay and CCK8 assay. The results from cell colony formation assay showed that ectopic expression of PTPN4 significantly depressed the clonogenicity of DLD-1 cells (Figure 3A,B) and NCM460 cells (Figure 3C,D) compared with the control cells. Moreover, the cell proliferation ability was remarkably suppressed in PTPN4-overexpressed DLD-1 cells (Figure 3E) and NCM460 cells (Figure 3F). To further confirm the influence of PTPN4 on the viability of CRC cells, we knock down endogenous expression of PTPN4 in DLD-1 cells by shRNA targeting the PTPN4. The RT-PCR and western blot assays showed that the PTPN4 were efficiently knocked down by the shRNA (Figure 3G,H). Consistently, the knockdown of PTPN4 dramatically boosted the clonogenicity (Figure 3I,J) and accelerated the cell growth (Figure 3K) in DLD-1 cells. In addition, we knocked out the PTPN4 gene in NCM460 via CRISPR/Cas9 system (Figure 3L,M). The data demonstrated that loss of PTPN4 similarly boosted the cell clonogenicity (Figure 3N,O) and accelerated the cell growth in NCM460 cells (Figure 3P). To further explore whether loss of PTPN4 had influence on the tumorigenesis, a tumor formation assay was performed with PTPN4 knockout NCM460 cells in vivo. We found that deletion of PTPN4 in NCM460 cells promoted the tumor formation (tumor was developed in 2 of 17 mice with implantation of $PTPN4^{KO}$ NCM460 cells), whereas the wild type of NCM460 cells could not form any tumors (Figure 3Q). Moreover, the histopathological examination showed that the tumors had morphological characteristics of poorly differentiated adenocarcinomas. (Figure 3R). Taken together,

FIGURE 2 Low expression of PTPN4 is associated with poor prognosis in rectal cancer. A, Approximately 27% (3 in 11 samples) of primary rectal cancer tissues showed a significant downregulation of PTPN4, while approximately 36% (4 in 11 samples) of the primary rectal cancer tissues exhibited high expression of PTPN4, compared with their adjacent normal tissues. A western blot assay was used to detect the PTPN4 protein level and PCNA was used to indicate the tumor tissues. GAPDH was used as a loading control. B, Patients with downregulated expression of PTPN4 (blue color) had more metastatic nodes. C, Immunohistochemical staining detected PTPN4 expression in tumor tissues of patients with stage II and III rectal cancer. 1: PTPN4 negative staining; 2: PTPN4 weak staining; 3: PTPN4 moderate staining; 4: More abundant expression of PTPN4 was observed in well-differentiated tumor tissue compared to poorly differentiated tumor tissue in the same slide. D, Patients with PTPN4 negative cytoplasm staining were more prone to lymphatic metastasis (P = 0.0153). E, The mRNA level of PTPN4 in tumors was remarkably increased compared with their paired adjacent normal tissues. Data were from the TCGA READ cohort and a paired Student's t test was used to analyze the statistical significance between the tumor tissues and the paired normal tissues (P = 0.0277). F, The mRNA level of PTPN4 was significantly increased in tumor tissues compared with normal tissues. Data were from the TCGA READ cohort and a Student's t test analysis was used to examine the significance between the tumor and the normal tissues. (P = 0.0015). G, The low expression of PTPN4 is associated with poor overall survival in rectal cancer. Data were from TCGA database, Rectal cancer patients were ranked according to PTPN4 mRNA level. The top 25% (High) and bottom 25% (Low) of patients were kept. Kaplan-Meier analysis was used to examine the survival rate (P = 0.014)

(A)

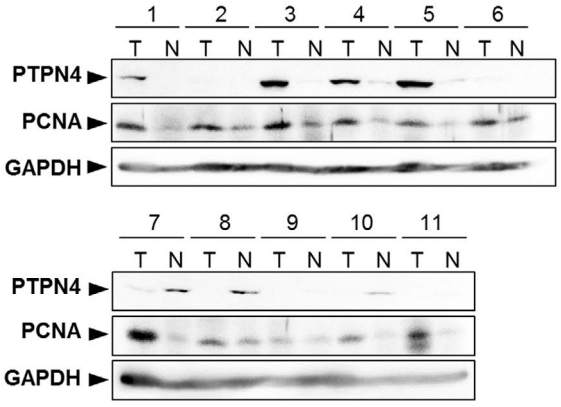

(B)

Number	Age	Sex	T*	N*
1	48	Female	T2	0/14
2	51	Female	T3	0/14
3	53	Female	T3	1/13
4	56	Male	T3	0/16
5	49	Female	T3	0/20
6	64	Female	T3	0/11
7	69	Male	T2	3/14
8	69	Female	T2	4/23
9	64	Male	T3	0/13
10	77	Male	T3	8/13
11	65	Female	T4	3/14

N, number of metastatic nodes/total number of lymph nodes detected; T, T staging according to NCCN Guidelines Version 1.2018.

(C)

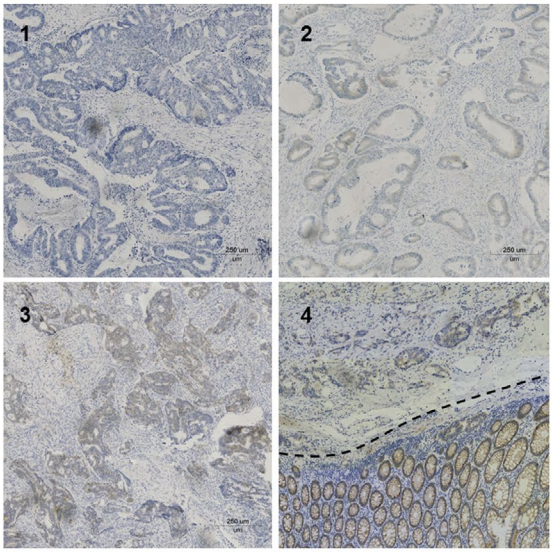

(D)

	PTPN4 expression		*P*-value
	Negative	Positive	
Tumor			0.5931
T2	2	0	
T3	25	13	
T4	7	3	
TNM stage			0.0153[b]
II	13	12	
III	21	4	
Lymph node metastasis			0.0153[b]
Negative	13	12	
Positive	21	4	

TNM staging according to NCCN Guidelines Version 1.2018; [b]$P < 0.05$.

(E)

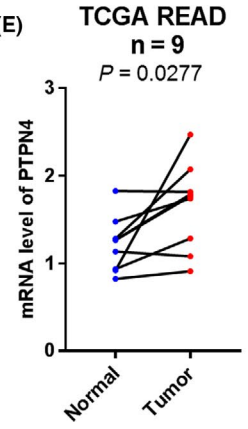

(F)

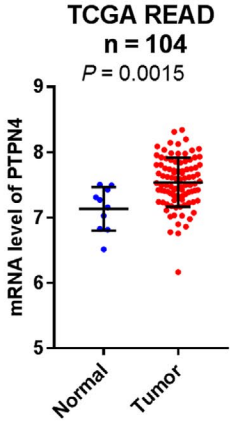

(G)

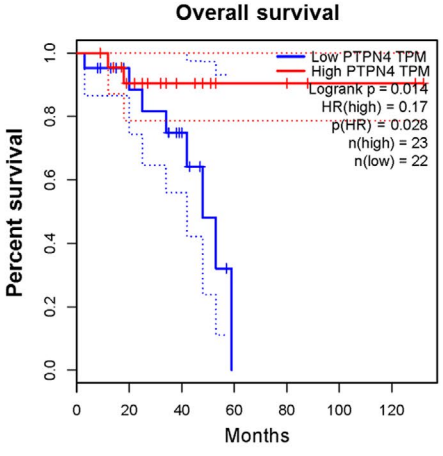

all these results lead us to the conclusion that PTPN4 suppresses the proliferation ability and tumorigenesis of colorectal cancer cells.

3.4 | Expression of PTPN4 correlates with cell cycle progression

Moreover, a FACS analysis was conducted to determine whether PTPN4 alters the cell cycle. Our cell cycle analysis clearly demonstrated that exogenous expression of PTPN4 shortened the S phase and prolonged the G1 phase in HEK293T cells (Figure 4A,B). Previously, we have found that downregulated PTPN4 promoted the colony formation and cell growth of colorectal cancer cells. To question whether PTPN4 had influence on the cell cycle, a FACS experiment was done to analyze the cell cycle of PTPN4 knockdown DLD-1 cells. Interestingly, knockdown of PTPN4 significantly promoted cells entering into the S phase from the G1 phase (Figure 4C,D), leading to an accelerated cell cycle. To further confirm this phenomenon, we examined the cell cycle variation of the PTPN4 deleted NCM460 cells. Consistently, we found that deletion of PTPN4 led to the short G1 phase and the arrest of G2/M phase (Figure 4E,F). These results indicate that loss of PTPN4 can accelerate the cell cycle of CRC cell lines.

3.5 | PTPN4 suppresses the transcription activities of STAT3 and Erk1/2 by impairing the levels of pSTAT3 (705) and pErk

Many studies have reported that PTPN4 is a PTP. To address the function of PTPN4 on overall state of protein tyrosine phosphorylation, we transfected HEK293T cells with 3HA-PTPN4 and conducted immunoprecipitation experiments. Overexpression of PTPN4 did not result in detectable changes in the overall state of protein tyrosine phosphorylation in lysate and co–immunoprecipitation product (Figure 4A). Previous studies showed that the endogenous PTPN4 only accounts for approximately 1/3000th of the total tyrosine phosphatase activity in COS-7 cells.[6] These results illustrated that the effect of PTPN4 on cell proliferation is likely via specific substrates rather than global dephosphorylation.

Previously, our laboratory demonstrated that PTPMeg2 directly mediates the dephosphorylation of pSTAT3 and negatively regulates STAT3 activity.[11] In other studies, PTPN2, PTPN3, PTPN5, PTPN7 and PTPN11 were reported to act on kinases upstream or downstream in EGF receptor-mediated signaling pathway. Therefore, we examined whether PTPN4 dephosphorylates STAT3 and Erk1/2. The results showed that the level of pSTAT3 (705) and pErk1/2 was decreased in a dose-dependent pattern when PTPN4 was overexpressed (Figure 5B) with or without EGF treatment. To evaluate whether the C-terminal deletion of PTPN4 had responsibility for the dephosphorylation function of PTPN4, we also transfected HEK293T with wild-type PTPN4 and PTPN4 $^{c.549dupT}$ under EGF treatment for 5 minutes after a starvation for 24 hours. PTPN4 c.549dupT failed to depress the level of pSTAT3 (705) and pErk1/2; however, the wild-type PTPN4 maintained the dephosphorylation ability for STAT3 and Erk1/2 (Figure 5C) Interestingly, PTPN4 leads to the decrease of phosphorylation of STAT3 at residue Try705 while having no impact on the phosphorylation of STAT3 at residue Ser727 (Figure 5C). These results suggested that overexpression of PTPN4 regulates the tyrosine phosphorylation of STAT3 and Erk1/2. To confirm whether PTPN4 interacted with STAT3 and Erk1/2 directly, PTPN4 and STAT3 were co–expressed in HEK293T cells and co–immunoprecipitation experiments were conducted. The results indicated that PTPN4 interacted with STAT3 and did not interact with STAT3 (Tyr705F) in vitro (Figure 5D). However, we did not detect the direct interaction between PTPN4 and Erk1/2 (data not shown). Immunostaining showed that PTPN4 localizes to the cytoplasm and cytomembrane (Figure 5E red). STAT3 localizes to the cytoplasm and nucleus (Figure 5E green). PTPN4 co–localized with STAT3 in the cytoplasm (Figure 5E merge). To address whether PTPN4 regulated the transcriptional activity of STAT3, we used an APRE luciferase reporter to examine the effect of PTPN4

FIGURE 3 PTPN4 suppresses the proliferation ability of colorectal cancer cells. A,B, Overexpression of PTPN4 inhibits the colony formation of DLD1 cells. Colonies formed by DLD1 cells overexpressing Flag-PTPN4 were stained with crystal violet (A) and counted in 3 independent experiments (B). For each well, 1000 cells were seeded into 6-well plates and allowed to grow for 10 d. EV represented the control cells with empty vector. $^{**}P < 0.01$. (C,D) Overexpression of PTPN4 suppresses the cell colony formation of NCM460 cells. 1000 of NCM460 cells with overexpression of Flag-PTPN4 and its control cells (EV) were seeded and stained with crystal violet 10 d later (C). Colonies were quantitated from 3 independent experiments (D). $^{*}P < 0.05$. (E,F) The cell viability is suppressed by PTPN4 exogenous overexpression in DLD1 (E) and NCM460 (F) cells. A CCK assay was performed with PTPN4 overexpressed cells and its control cells (EV). The cell viability was presented as OD450 values. G,H, DLD1 cell-based stable cell lines for knocking down of PTPN4 by shRNA. RT-PCR (G) and western blot (H) experiments were used to examine the knockdown efficiency in stable cell lines established by lentivirus infection. GAPDH was used as a loading control. (I-J) Knocking down of PTPN4 promotes the colony formation. DLD1 knocking down and its control cells (shNC) were used for the colony formation assay (I). A quantitative presentation of colonies from 3 independent experiments is shown (J). K, The cell proliferation ability is enhanced by depletion of PTPN4. A CCK8 assay was performed with PTPN4 knocking down DLD1 and its control cells. (L,M) An NCM460 stable cell line for PTPN4 deletion. NCM460 cells were used to genetically delete PTPN4 by a CRISPR/Cas9 system. RT-PCR (L) and western blot (M) showed the complete deletion of endogenous expression of PTPN4. (N,O) Deletion of PTPN4 inhibits colony formation in NCM460 cells. Wild-type (Control) and PTPN4 deletion (PTPN4-KO) cells based on NCM460 cell line were examined for the colony formation assay (N). A quantitative presentation of colonies from 3 independent experiments is shown (O). P, The proliferation ability is significantly increased by PTPN4 deletion compared with the control cells. Wild-type (Control) and PTPN4 deletion (PTPN4-KO) cells based on NCM460 cell line were used for the CCK assay. Q, Deletion of PTPN4 promotes the tumorigenesis of NCM460 cells. The tumor formation assay was performed by bilaterally injecting 1×10^7 wild-type and PTPN4 deleted NCM460 cells into the armpit of BALB/c nude mice. R, The tumor was from (Q) and identified by the morphology with H&E staining. The tumor has morphological characteristics of poorly differentiated adenocarcinomas

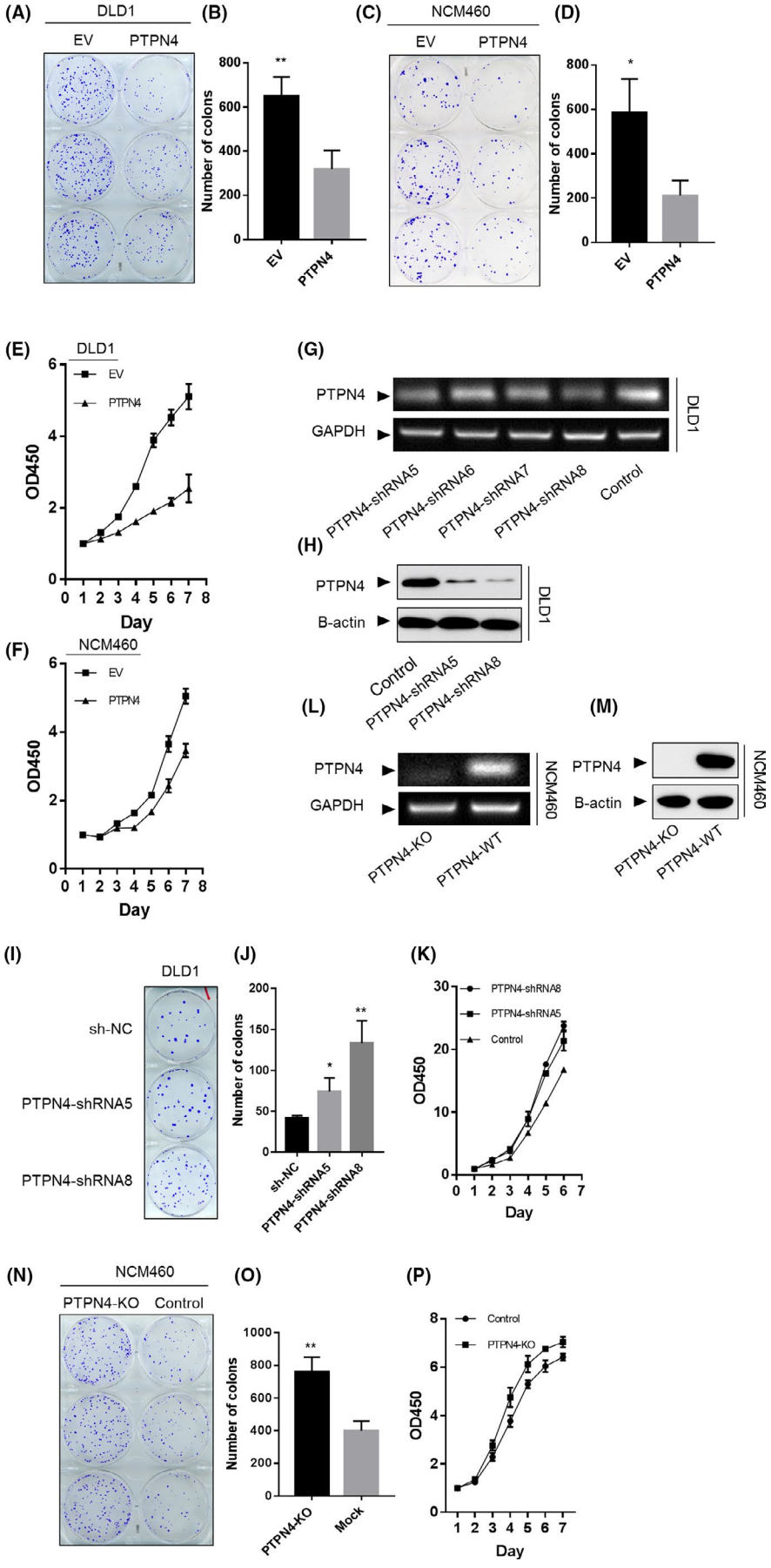
(A)
DLD1
EV
PTPN4
(B)
Number of colons
800
600
400
200
0
**
EV
PTPN4
(C)
NCM460
EV
PTPN4
(D)
Number of colons
800
600
400
200
0
*
EV
PTPN4
(E)
DLD1
EV
PTPN4
OD450
6
4
2
0
0 1 2 3 4 5 6 7 8
Day
(F)
NCM460
EV
PTPN4
OD450
6
4
2
0
0 1 2 3 4 5 6 7 8
Day
(G)
PTPN4
GAPDH
DLD1
PTPN4-shRNA5
PTPN4-shRNA6
PTPN4-shRNA7
PTPN4-shRNA8
Control
(H)
PTPN4
B-actin
DLD1
Control
PTPN4-shRNA5
PTPN4-shRNA8
(L)
PTPN4
GAPDH
NCM460
PTPN4-KO
PTPN4-WT
(M)
PTPN4
B-actin
NCM460
PTPN4-KO
PTPN4-WT
(I)
DLD1
sh-NC
PTPN4-shRNA5
PTPN4-shRNA8
(J)
Number of colons
200
150
100
50
0
*
**
sh-NC
PTPN4-shRNA5
PTPN4-shRNA8
(K)
PTPN4-shRNA8
PTPN4-shRNA5
Control
OD450
30
20
10
0
0 1 2 3 4 5 6 7
Day
(N)
NCM460
PTPN4-KO
Control
(O)
Number of colons
1000
800
600
400
200
0
**
PTPN4-KO
Mock
(P)
Control
PTPN4-KO
OD450
8
6
4
2
0
1 2 3 4 5 6 7
Day

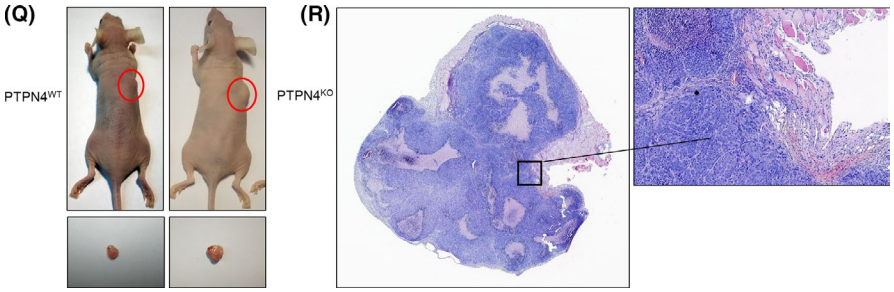

FIGURE 3 (Continued)

on STAT3-mediated transcriptional activity. The results indicated that overexpression of PTPN4 in HEK293T cells results in a decrease of the luciferase activity in response to stimulation of EGF (Figure 5F). We also found that the PTPN4 abrogated the inducible transcriptional activity of Erk1/2 treated with EGF in HEK293T cells (Figure 5G). Then, we conducted cytokine addition-withdrawal assays in NCM460 cells. Western blot analysis showed that pSTAT3 (705) remained significantly stronger when EGF was withdrawn after stimulation for 5 minutes in PTPN4-deleted NCM460 cells compared with PTPN4 wild-type cells, while scarcely any change was observed for pErk1/2 (Figure 5H). Does PTPN4 affect the distribution of STAT3 in colorectal epithelial cells? We used $PTPN4^{KO}$ NCM460 cell line to monitor the dynamic distribution of STAT3 in cells by immunofluorescence assay. After 24-hour serum-free starvation, EGF (25 ng/mL) stimulated $PTPN4^{KO}$ cell line and $PTPN4^{WT}$ cell line for 5 minutes. Then cells were cultured in new serum-free medium for 0, 10, 20 and 30 minutes. We found that STAT3 began to enter the nucleus after EGF treatment. After 10 minutes of EGF withdrawal, STAT3 was concentrated in the nucleus of the 2 kinds of cells. After 20 minutes of EGF withdrawal, STAT3 began to decrease in the nucleus of the $PTPN4^{WT}$ cell line. After 30 minutes of EGF withdrawal, STAT3 in $PTPN4^{KO}$ cell line was still concentrated in the nucleus while more STAT3 was found in the cytoplasm than in the nucleus in $PTPN4^{WT}$ cell line. All the results suggested that PTPN4 could repress STAT3 and Erk1/2 transcriptional activity and dephosphorylate pSTAT3 (705).

4 | DISCUSSION

Most CRC occurs sporadically due to genetic mutations and epigenetic modifications of the human genome.[12] These genetic mutations and epigenetic modifications promote the conversion from normal mucosa toward carcinoma by altering signaling pathways such as Ras/ERK1/2, Src, JAK/STAT, JNK, NF-κB, Wnt and PTEN/PI3K/AKT. In 1990, Vogelstein proposed a multistep carcinogenesis model of CRC from normal colonic epithelium to adenocarcinoma.[13] This model involves genetic mutations in several genes, such as loss of function in the APC gene, which was considered as an early event of multistep carcinogenesis.

Protein tyrosine phosphatases belong to a super family of enzymes that includes more than 100 genes.[3,14] PTPs are classified into 2 groups according to their function: tumor suppressor PTPs and oncogenic PTPs. The loss of function in tumor suppressor PTPs is often observed in cancer due to gene mutations, deletions and epigenetic modifications. Loss of these tumor suppressor PTPs leads to hyperactivation in some signaling pathways and promotes tumorigenesis. Product of the wild-type form of these genes depresses the growth of colorectal cancer cells.[15] Mutations leading to loss of function in non–receptor PTPs, including PTPN3, PTPN13 and PTPN14, were identified in several human cancers (including gastric, lung, breast and colorectal cancer). However, whether PTPN genes are responsible for the development of colorectal cancer still needs to be explored and the detailed mechanism remains to be elucidated.

In our study, we identified a nonsense mutation of PTPN4 from 1 case of rectal cancer with a mutation ratio of 90.90%. The mutation ratio exceeded 50%, so PTPN4 c.549dupT was a biallelic mutation. Biallelic mutations are less common in somatic mutations. How did this somatic mutation turn into a biallelic mutation? We proposed a model. Homologous recombination (HR) can promote the exchange of DNA sequence information between homologous regions in a genome. If the interacting sequences in HR are heterozygous, this information transfer results in the transformation from heterozygous gene to homozygous gene. After PTPN4 got c.549dupT mutation, HR following DNA damage helped PTPN4 c.549dupT turn into a biallelic mutation. This mutation led to loss of function in the PTPN4 gene, which is similar to the report of loss of activity of PTPN13 through somatic mutations in some tumors.[16] The ratio of 90.90% indicated

FIGURE 4 The expression of PTPN4 correlates with the cell cycle progression. (A,B) Exogenous expression of PTPN4 shortens the S phase and prolongs the G1 phase in HEK293T cells. The PTPN4 overexpression (PTPN4) and its control cells (EV) were stained with propidium iodide and the cell cycle was examined by FACS (A). A quantitative presentation of cell phases from 3 independent experiments and the Student's *t* test was used for the significance analysis (B). $^{*}P < 0.05$, $^{**}P < 0.01$, $^{***}P < 0.001$. (C,D) Depletion of PTPN4 significantly promotes cells enter into the S phase from the G1 phase. The cell cycle of PTPN4 knocking down (PTPN4-shRNA5/8) and its control cells were examined by FACS (C). A quantitative presentation of cell phases from 3 independent experiments (D). $^{*}P < 0.05$, $^{**}P < 0.01$, $^{***}P < 0.001$. (E,F) Deletion of PTPN4 leads to the shortened G1 phase and the arrest of G2/M. A FACS was used to determine the cell phases of PTPN4 deletion ($PTPN4^{KO}$) and its control cells (mock) (E). A quantitative presentation of the cell phases from 3 independent experiments (F). $^{**}P < 0.01$, $^{***}P < 0.001$

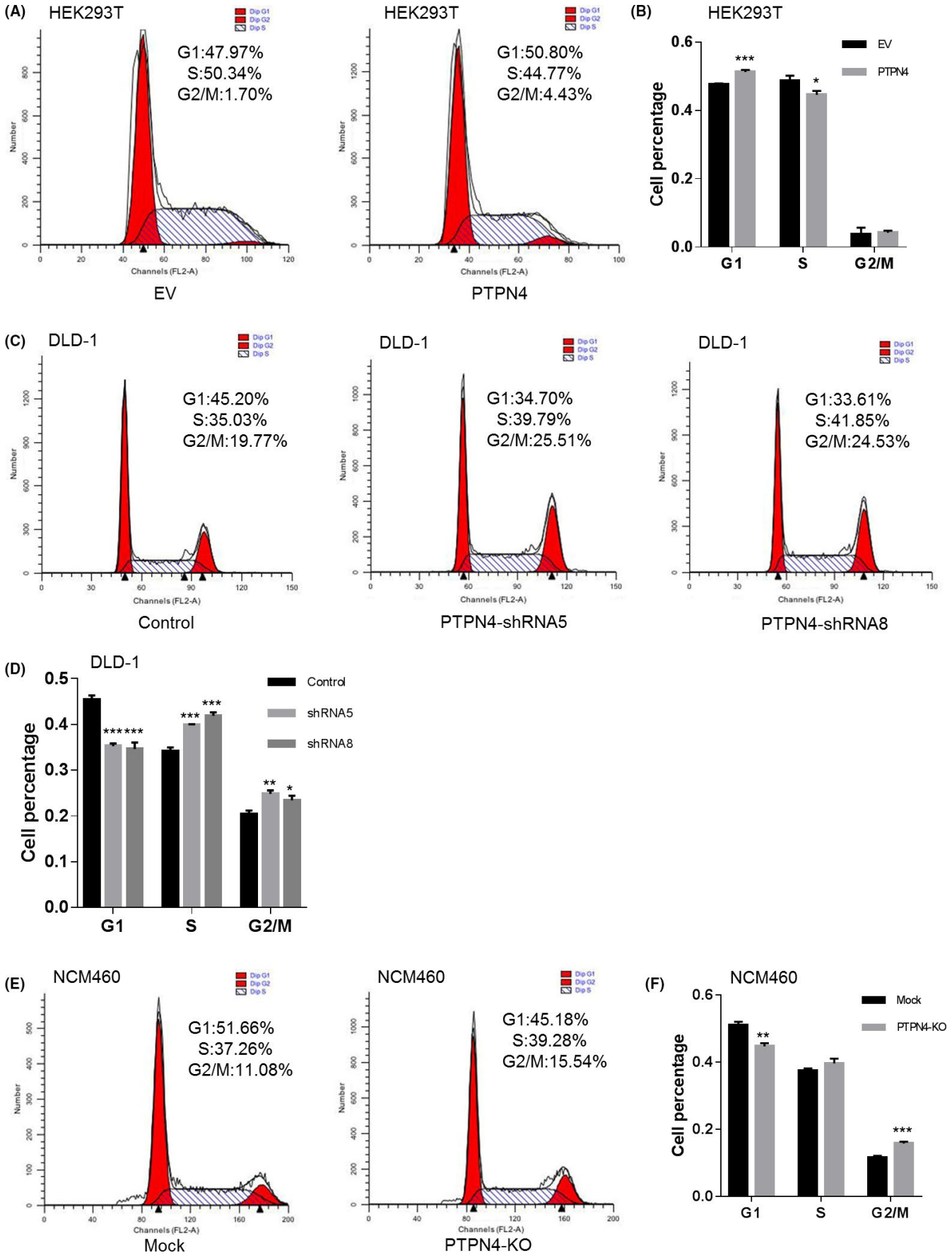
(A)
HEK293T
G1:47.97%
S:50.34%
G2/M:1.70%
EV
HEK293T
G1:50.80%
S:44.77%
G2/M:4.43%
PTPN4
(B)
HEK293T
EV
PTPN4
Cell percentage
G1
S
G2/M
(C)
DLD-1
G1:45.20%
S:35.03%
G2/M:19.77%
Control
DLD-1
G1:34.70%
S:39.79%
G2/M:25.51%
PTPN4-shRNA5
DLD-1
G1:33.61%
S:41.85%
G2/M:24.53%
PTPN4-shRNA8
(D)
DLD-1
Control
shRNA5
shRNA8
Cell percentage
G1
S
G2/M
(E)
NCM460
G1:51.66%
S:37.26%
G2/M:11.08%
Mock
NCM460
G1:45.18%
S:39.28%
G2/M:15.54%
PTPN4-KO
(F)
NCM460
Mock
PTPN4-KO
Cell percentage
G1
S
G2/M

that this mutation may be an early event of multistep carcinogenesis in this CRC patient. To investigate whether loss of PTPN4 leads to the occurrence of colorectal cancer, we performed a tumorigenesis assay by injecting NCM460 into BALB/c nude mice (Figure 3Q). The results showed that the deletion of PTPN4 caused 2/17 of the mice to develop tumors, whereas no tumor was generated by the wild-type NCM460 cells (Figure 3Q). A further histopathological examination showed that the tumor had morphological characteristics of poorly differentiated adenocarcinomas. (Figure 5R). Meanwhile, as a normal immortalized cell line, in other experiments in our laboratory, wild-type NCM460 cell line cannot grow tumor in nude mice (data not shown). Therefore, our results illustrated that loss of PTPN4 increases the risk of tumorigenesis.

Mutations of PTPN4 were detected in human colorectal cancer tissues with a ratio of 3.65% from the TCGA READ database and upregulation of PTPN4 mRNA was also observed in rectal cancer samples compared with normal samples from the TCGA READ cohort (Figures 1F and 2E,F). However, low expression of PTPN4 in rectal cancer is associated with poor prognosis (Figure 2G). All these results suggested that significant alteration of PTPN4 in genomic and transcriptional level does not occur frequently. PTPN4 may not be a driver gene in most rectal cancers. We explored the function of PTPN4 in CRC and found that overexpression of PTPN4 suppressed the cell growth and clonogenicity of colorectal cancer cells. Meanwhile, the cell cycle analysis by FACS indicated that the G1 phase was shortened and the S phase was prolonged when PTPN4 was deleted in NCM460 cells, leading to elevated cell cycle process. These results imply that loss of PTPN4 promoting the cell viability might be through the alteration of the cell cycle. However, understanding the detailed signal pathways of PTPN4 involved into the cell cycle requires further study.

In terms of the molecular mechanism, we found that PTPN4 is a tumor repressor dephosphorylating pSTAT3 at residue Tyr705 but not Ser727, leading to suppressed transcriptional activity of STAT3. Hyperphosphorylation of STAT3 at residue Tyr705 is associated with different kinds of human cancers.[17] Phosphorylated STAT3 dimerizes and accumulates in the nucleus, where it activates the transcription of a series of genes, including c-Myc and cyclin D1.[18] Loss of PTPN4 leads to the hyperactivation of STAT3 signaling pathway and promotes tumorigenesis. Interestingly, we also found that PTPN4 interacted with STAT3 and did not interact with STAT3 (Tyr705F) in vitro (Figure 5D). However, even though the decreased phosphorylation of Erk was observed in PTPN4 overexpressed cells (Figure 5B,C), the interaction between PTPN4 and Erk1/2 could not be examined. Moreover, we found that the phosphorylation level of Erk1/2 was scarcely changed in the PTPN4-deleted NCM460 cells when EGF was withdrawn after stimulation for 5 minutes, while pSTAT3 remained significantly stronger at the same time in a cytokine addition-withdrawal assay (Figure 5H). Nevertheless, the overexpression of PTPN4 resulted in a decrease of the transcriptional activity of Erk1/2 in response to stimulation of EGF (Figure 5G). We hypothesize that the regulation of PTPN4 on Erk may be through other factors in an indirect manner, which remains to be explored in the future. Although we have demonstrated that PTPN4 participated in the regulation of

FIGURE 5 PTPN4 suppresses the transcription activities of STAT3 and Erk by impairing the levels of pSTAT3 and pErk. A, No detectable changes of the tyrosine phosphorylation were observed for the overall state of proteins in PTPN4 overexpressed HEK293T cells compared with the control group. 3HA-PTPN4 was transfected into HEK293T cells and immunoprecipitation (IP) was performed using an antibody against HA after 24 h of transfection. The precipitation complex was examined bywestern blot using an antibody against HA (left) or anti–phosphotyrosine antibody (4G10) (right). The tyrosine phosphorylation of total cell lysate was detected by western blot with a 4G10 antibody (right, the first and second lanes). (B) PTPN4 robustly suppresses the phosphorylation level of pSTAT3 (Tyr705) and pErk1/2 with or without epidermal growth factor (EGF; 25 ng/mL) treatment for 5 min in a dose-dependent manner. Different amounts of 3HA-PTPN4 were transfected into HEK293T cells and western blot was performed with the indicated antibodies. β-actin was used as a loading control. (C) Wild-type, but not the truncated, PTPN4 suppresses the phosphorylation of pSTAT3 (Tyr705) and pErk1/2 in the presence of EGF (25 ng/mL) for 5 min. The 3Flag-PTPN4 and 3Flag-PTPN4$^{c.549dupt}$ were transfected into HEK293T cells and levels of pSTAT3 (Tyr705), pSTAT3 (Ser727) and pErk1/2 were examined with western blot in the presence of EGF (25 ng/mL) for 5 min. (D) PTPN4 specifically interacts with STAT3 in vitro. Flag-STAT3 and 3HA-PTPN4 (or Flag-STAT3 (Tyr705F) and 3HA-PTPN4) were transfected into HEK293T cells and harvested for the precipitation after 24-36 h. Immunoprecipitation (IP) was performed using an antibody against Flag or HA. The complex was examined by a western blot using antibody against Flag and HA. The lysate and precipitated complex were examined by a western blot using antibodies against HA and Flag. E, PTPN4 co–localizes with STAT3 in the cytoplasm. HEK293T cells expressing 3Flag-PTPN4 were stained with an anti–Flag (red) and STAT3 (green) antibody. The images were viewed with a confocal microscope. Colocalization of 3Flag-PTPN4 and STAT3 in the cytoplasm is shown as yellow. F, PTPN4 abrogates the inducible transcriptional activity of STAT3 treated with EGF. Luciferase assays were performed using HEK293T cells with transient expression of 3HA-PTPN4 with APRE-Luc. The pRL-TK was used as an internal control. G, PTPN4 inhibits EGF-stimulated transcriptional activity of Erk1/2. The 3HA-PTPN4 was co–transfected with pFA-luc and pFR-ELK1 plasmids into HEK293T cells for the luciferase experiment. The pRL-TK was used as an internal control. Student's *t* test was used for the significance analysis for the luciferase assay. ***$P < 0.001$. Results are showed as mean ± SD from 3 independent experiments. H, Deletion of PTPN4 impairs the dephosphorylation of pSTAT3 and pErk1/2. Wild-type PTPN4 (PTPN4^{WT}) and PTPN4 knockout (PTPN4^{KO}) NCM460 cells were treated with EGF (25 ng/mL) for 5 min, followed by releasing into serum-free medium for the indicated times. The cell lysate was detected by anti–pSTAT3 (Tyr705) and anti–pErk1/2 antibodies with western blot and the β-actin was used as a loading control. (I) Immunofluorescence staining showed that STAT3 stayed longer in the nucleus in PTPN4^{KO} NCM460 cells. Wild-type PTPN4 (PTPN4^{WT}) and PTPN4 knockout (PTPN4^{KO}) NCM460 cells were treated with EGF (25 ng/mL) for 5 min, followed by releasing into serum-free medium for indicated times. Then cells were fixed with 4% paraformaldehyde for 20 min and perforated with .3% Triton X-100 for 10 min. After blocking with 10% FBS for 50 min, cells were incubated with anti–STAT3 antibody overnight at 4°C, followed with incubation with the second antibody coupled with green fluorescence, then stained with DAPI

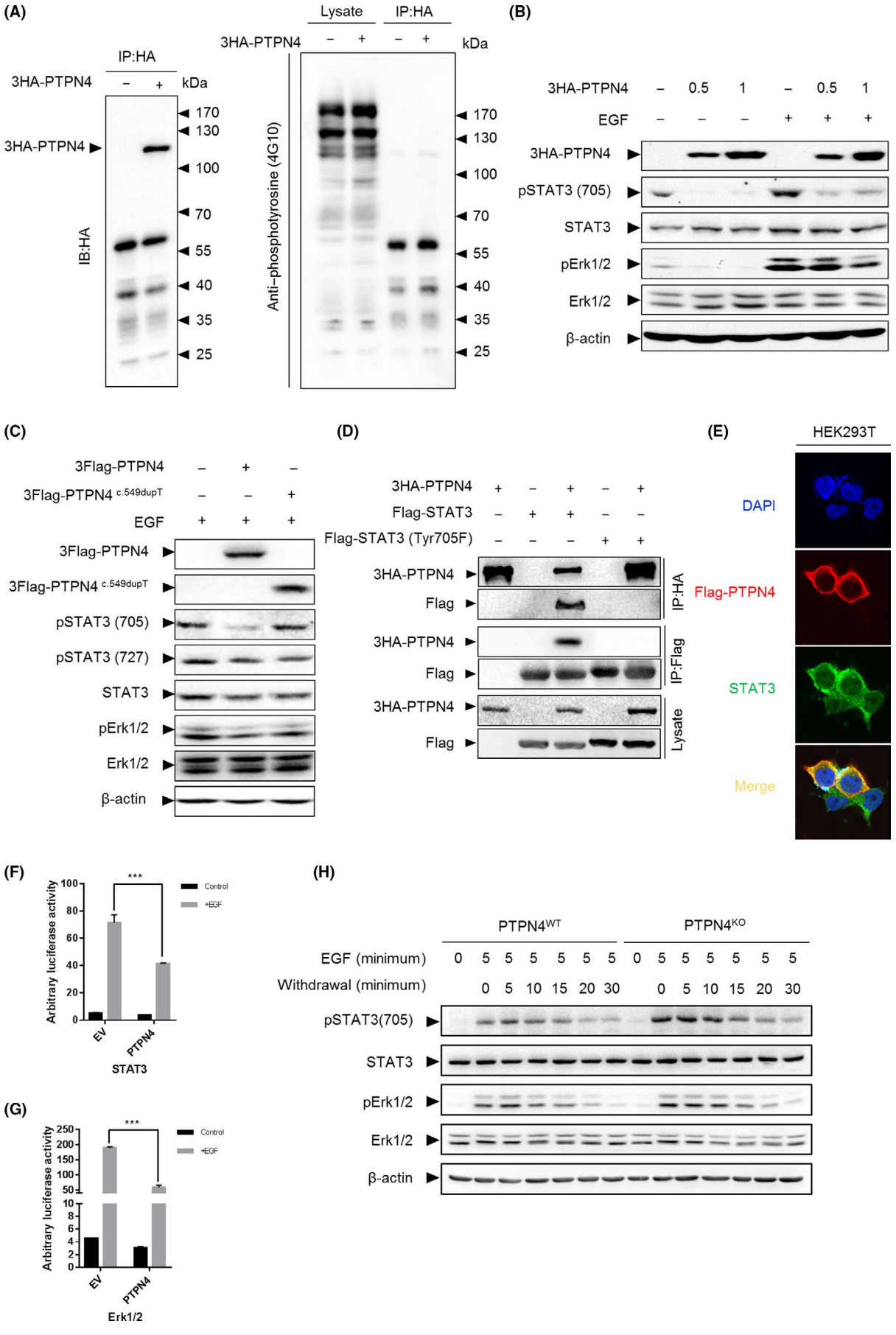
(A)
IP:HA
3HA-PTPN4
kDa
170
130
100
70
55
40
35
25
IB:HA
Lysate
IP:HA
Anti–phosphotyrosine (4G10)
(B)
EGF
pSTAT3 (705)
STAT3
pErk1/2
Erk1/2
β-actin
(C)
3Flag-PTPN4
3Flag-PTPN4 c.549dupT
EGF
pSTAT3 (727)
(D)
Flag-STAT3
Flag-STAT3 (Tyr705F)
Flag
IP:HA
IP:Flag
Lysate
(E)
HEK293T
DAPI
Flag-PTPN4
STAT3
Merge
(F)
Arbitrary luciferase activity
Control
+EGF
EV
PTPN4
STAT3
(G)
Erk1/2
(H)
PTPN4WT
PTPN4KO
EGF (minimum)
Withdrawal (minimum)
pSTAT3(705)

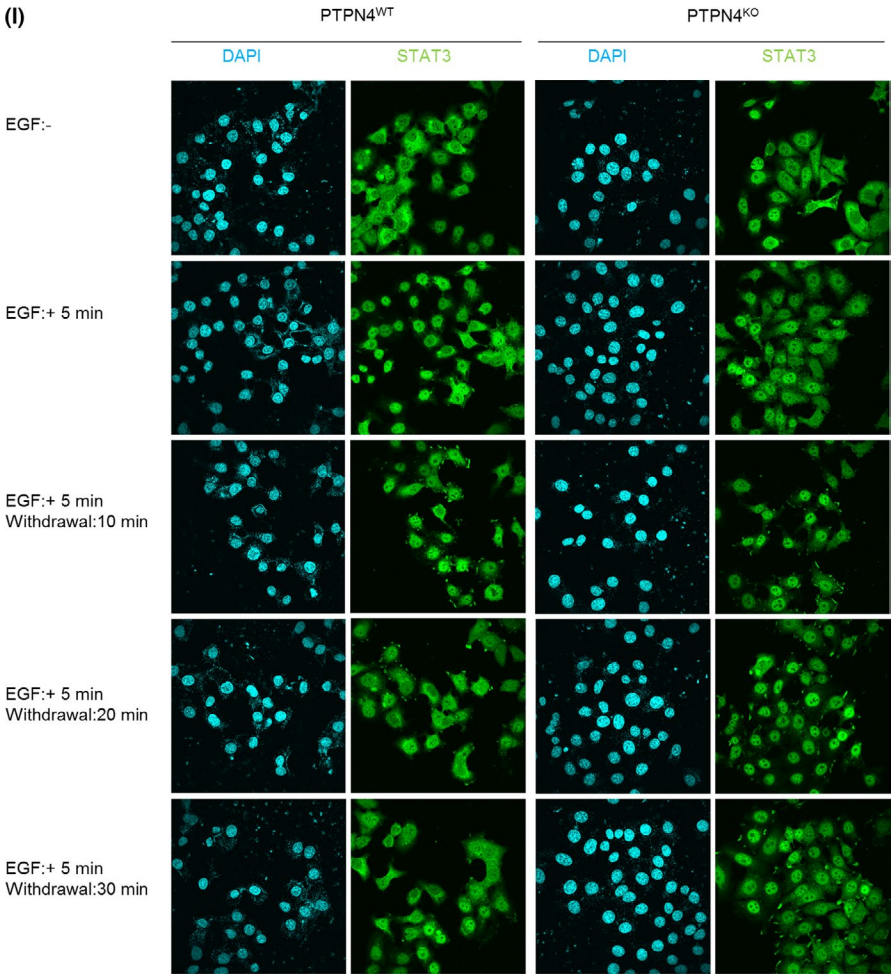

FIGURE 5 (Continued)

STAT3 and Erk, we cannot exclude the possibility that PTPN4 may target other substances, based on the fact that PTPN4 was shown to participate in many biological processes.

Currently, whole-exome sequencing and integrative analysis of genomic data provide insight into the pathways that are dysregulated in CRC. Most studies focus on somatic mutation frequencies in the population. However, the mutation ratio in 1 sample can also provide a lot of information about the function of somatic mutation on tumorigenesis and tumor progression. In our study, we identified that a nonsense mutation of PTPN4 resulted in a loss of function for the wild-type gene and revealed the mechanism that deletion of PTPN4 promotes the cell proliferation and tumorigenesis in CRC through the regulation of pSTAT3 and pErk, which might be a novel target for the therapy of CRC.

DISCLOSURE

We declare that we have no financial and personal relationships with other people or organizations that can inappropriately influence our work, there is no professional or other personal interest of any nature or kind in any product, service and/or company that could be construed as influencing the position presented in, or the review of, the manuscript entitled "Loss of PTPN4 Activates STAT3 to Promote the Tumor Growth in Rectal Cancer."

ORCID

Bing-Dong Zhang https://orcid.org/0000-0003-2911-7192

REFERENCES

1. Cancer Genome Atlas Network. Comprehensive molecular characterization of human colon and rectal cancer. *Nature*. 2012;487:330-337.
2. Ostman A, Bohmer FD. Regulation of receptor tyrosine kinase signaling by protein tyrosine phosphatases. *Trends Cell Biol*. 2001;11:258-266.
3. Alonso A, Sasin J, Bottini N, et al. Protein tyrosine phosphatases in the human genome. *Cell*. 2004;117:699-711.
4. Gu MX, York JD, Warshawsky I, Majerus PW. Identification, cloning, and expression of a cytosolic megakaryocyte protein-tyrosine-phosphatase with sequence homology to cytoskeletal protein 4.1. *Proc Natl Acad Sci USA*. 1991;88:5867-5871.
5. Gu M, Majerus PW. The properties of the protein tyrosine phosphatase PTPMEG. *J Biol Chem*. 1996;271:27751-27759.
6. Gu M, Meng K, Majerus PW. The effect of overexpression of the protein tyrosine phosphatase PTPMEG on cell growth and on

colony formation in soft agar in COS-7 cells. *Proc Natl Acad Sci USA*. 1996;93:12980-12985.
7. Zhou J, Wan B, Shan J, Shi H, Li Y, Huo K. PTPN4 negatively regulates Crkl in human cell lines. *Cell Mol Biol Lett*. 2013;18:297-314.
8. Kina S, Tezuka T, Kusakawa S, et al. Involvement of protein-tyrosine phosphatase PTPMEG in motor learning and cerebellar long-term depression. *Eur J Neurosci*. 2007;26:2269-2278.
9. Kohda K, Kakegawa W, Matsuda S, Yamamoto T, Hirano H, Yuzaki M. The delta2 glutamate receptor gates long-term depression by coordinating interactions between two AMPA receptor phosphorylation sites. *Proc Natl Acad Sci USA*. 2013;110:E948-E957.
10. Jin M, Frankel WL. Lymph node metastasis in colorectal cancer. *Surg Oncol Clin N Am*. 2018;27:401-412.
11. Su F, Ren F, Rong Y, et al. Protein tyrosine phosphatase Meg2 dephosphorylates signal transducer and activator of transcription 3 and suppresses tumor growth in breast cancer. *Breast Cancer Res*. 2012;14:R38.
12. Lynch HT, de la Chapelle A. Hereditary colorectal cancer. *N Engl J Med*. 2003;348:919-932.
13. Fearon ER, Vogelstein B. A genetic model for colorectal tumorigenesis. *Cell*. 1990;61:759-767.
14. Andersen JN, Jansen PG, Echwald SM, et al. A genomic perspective on protein tyrosine phosphatases: gene structure, pseudogenes, and genetic disease linkage. *FASEB J*. 2004;18:8-30.
15. Wang Z, Shen D, Parsons DW, et al. Mutational analysis of the tyrosine phosphatome in colorectal cancers. *Science*. 2004;304:1164-1166.
16. Dromard M, Bompard G, Glondu-Lassis M, Puech C, Chalbos D, Freiss G. The putative tumor suppressor gene PTPN13/PTPL1 induces apoptosis through insulin receptor substrate-1 dephosphorylation. *Cancer Res*. 2007;67:6806-6813.
17. Yue P, Turkson J. Targeting STAT3 in cancer: how successful are we? *Expert Opin Investig Drugs*. 2009;18:45-56.
18. Inghirami G, Chiarle R, Simmons WJ, Piva R, Schlessinger K, Levy DE. New and old functions of STAT3: a pivotal target for individualized treatment of cancer. *Cell Cycle*. 2005;4:1131-1133.

SUPPORTING INFORMATION

Additional supporting information may be found online in the Supporting Information section at the end of the article.

How to cite this article: Zhang B-D, Li Y-R, Ding L-D, Wang Y-Y, Liu H-Y, Jia B-Q. Loss of PTPN4 activates STAT3 to promote the tumor growth in rectal cancer. *Cancer Sci*. 2019;110:2258–2272. https://doi.org/10.1111/cas.14031